DOI: 10.1002/ejic.201000392

Optical Properties and Energy Transfer of $NaCaPO_4:Ce^{3+},Tb^{3+}$ Phosphors for Potential Application in Light-Emitting Diodes

Ning Guo,[a,b] Yanhua Song,[a,b] Hongpeng You,*[a] Guang Jia,[a,b] Mei Yang,[a,b] Kai Liu,[a,b] Yuhua Zheng,[a,b] Yeju Huang,[a,b] and Hongjie Zhang*[a]

Keywords: Terbium / Cerium / Phosphors / Luminescence / Energy transfer

$NaCaPO_4:Ce^{3+},Tb^{3+}$ phosphors were prepared by a solid-state reaction. Their luminescence properties reveal that an efficient energy transfer from the Ce^{3+} to Tb^{3+} ions occurs, and its mechanism is a resonant type by means of a dipole–quadrupole reaction. The critical distance of the energy transfer has been calculated by concentration-quenching and spectral-overlap methods. The varied emitted color of the phosphors from blue to yellow-greenish can be achieved by properly tuning the relative ratio of Ce^{3+} and Tb^{3+} through the energy transfer from the Ce^{3+} to Tb^{3+} ions. These results indicate that $NaCaPO_4:Ce^{3+},Tb^{3+}$ is potentially useful as a highly efficient, green-emitting, UV-convertible phosphor for white-light-emitting diodes. Moreover, the accurate oscillator strength ratio of the electric quadrupole-to-dipole transitions for the Tb^{3+} ion was obtained to be about 10^{-3}, which may be of much significance in the estimate of the critical distance of the dipole–quadrupole interaction between Ce^{3+} and Tb^{3+} ions through Dexter's energy-transfer theory.

Introduction

White light-emitting diodes (LEDs) show high potential for replacement of conventional lighting such as incandescent and fluorescent lamps because of their long lifetime, higher energy efficiency, better reliability, and environmentally friendly characteristics.[1–3] Therefore, white-light LEDs are considered to be next-generation solid-state lighting devices. Currently, the most common approach to realize white-light LEDs is to combine an InGaN-based blue diode with yellow luminescence from a $Y_3Al_5O_{12}:Ce^{3+}$ (YAG:Ce) phosphor, although this approach faces problems of thermal quenching and poor color rendition.[4] As an alternative, the combination of a UV chip with red, green, and blue phosphors can generate warm white light.[5] Therefore, phosphor materials play an important role in white-light LEDs. However, most phosphors used at present do not meet the optimum requirements of white-light LEDs. Besides high conversion efficiency into visible light, the necessary requirement for the appropriate phosphors used for UV LEDs is a high quenching temperature, which is important for the phosphor used in phosphor-conversion white-light LEDs, because it has a great influence on the light output and color-rendering index. Therefore, it is necessary to develop novel phosphor materials that exhibit higher thermal stability for white-light LEDs. In this regard, thermally stable phosphate phosphors have been reported for white-light LEDs.[6–8]

In recent years, phosphate compounds have gained increasing interest in the investigations of new luminescent materials applied in white-light LEDs. $ABPO_4$ (in which A and B are mono- and divalent cations, respectively) compounds show excellent thermal and charge stability and are considered to be efficient luminescent hosts.[9] Hence there is an increased interest in the synthesis of new efficient luminescent materials that have structures derived from the $ABPO_4$ family. Recently, Eu^{2+}-activated $KSrPO_4$ phosphors with excellent thermal stabilities that emit strong blue light under UV-light irradiation have been reported.[10] Chan et al. also reported that the Mn^{2+}-doped green-yellow-emitting phosphor $LiZnPO_4$ had the potential for application as a phosphor in white-light LEDs.[11] It is well-known that a Ce^{3+} ion may act as a highly efficient emission center because the 4f–5d transitions of the Ce^{3+} ion are allowed by the Laporte parity selection rules. One strategy to enhance the luminescence of Tb^{3+} ions is to use the codoping of the Ce^{3+} ion as a sensitizer. Generally, Ce^{3+} is also an effective sensitizer for Tb^{3+} in many hosts, which encouraged us to consider the feasibility of the energy transfer between Ce^{3+} and Tb^{3+} in the $NaCaPO_4$ host. On the basis of the energy-transfer theory developed by Dexter,[12] the efficiency of the energy transfer depends mainly on the extent of overlap between the Ce^{3+} emission and the Tb^{3+} excitation spectra. The energy-transfer processes between Ce^{3+} and Tb^{3+} in different hosts have been extensively in-

[a] State Key Laboratory of Rare Earth Resource Utilization, Changchun Institute of Applied Chemistry, Chinese Academy of Sciences,
Changchun 130022, P. R. China
Fax: +86-431-85698041
E-mail: hpyou@ciac.jl.cn
hongjie@ciac.jl.cn
[b] Graduate University of the Chinese Academy of Sciences, Beijing 100049, P. R. China

Supporting information for this article is available on the WWW under http://dx.doi.org/10.1002/ejic.201000392.

vestigated.[13–18] The main interest has been in the development of new and highly efficient green-emitting phosphors for use as green components in white-light LEDs. In particular, terbium-ion-incorporated materials with four sharp emissions of the $^5D_4 \rightarrow {}^7F_J$ (J = 3, 4, 5, 6) transitions of the Tb^{3+} ions and a predominant $^5D_4 \rightarrow {}^7F_5$ transition that peaks at around 545 nm are utilized as green-emitting phosphors such as $LaPO_4$[19] and $CeMgAl_{11}O_{19}$.[20] The efficient green emission from these phosphors is due to the energy transfer from the Ce^{3+} to Tb^{3+} ions. The importance of the energy-transfer process in these phosphors has led to investigations into novel host materials for codoping Tb^{3+} ions along with Ce^{3+} ions. However, to the best of our knowledge, there is no report on the research of $NaCaPO_4:Ce^{3+},Tb^{3+}$ for its potential application as a green phosphor.

In the present study, we have investigated the luminescence, energy-transfer, and color-chromaticity properties of the $NaCaPO_4:Ce^{3+},Tb^{3+}$ phosphor. We have also calculated the energy-transfer critical distance between the Ce^{3+} and Tb^{3+} ions on the basis of the model proposed by Blasse.[21] The energy transfer from the Ce^{3+} to Tb^{3+} ions is also of a resonant type that takes place by means of a dipole–quadrupole mechanism, and the energy-transfer efficiencies were calculated by the changes in their relative emission intensity. Furthermore, we have demonstrated that $NaCaPO_4:Ce^{3+},Tb^{3+}$ phosphors can generate lights from the blue to yellow-greenish region under UV excitation by appropriately tuning the relative ratio of the Ce^{3+} and Tb^{3+} ions.

Results and Discussion

Phase Identification and Crystal Structure

Figure 1 shows the XRD patterns of $NaCaPO_4:0.02Ce^{3+},nTb^{3+}$ with different doping contents. All diffraction peaks were found to be in good agreement with that reported in the JCPDS file 29-1193, regardless of the contents of the dopants, thereby indicating that the obtained samples are single-phase and the codoped Ce^{3+} and Tb^{3+} ions do not cause any significant change in the host structure. On the basis of the effective ionic radii of cations with different coordination numbers,[22] we suggested that the Ce^{3+} and Tb^{3+} ions prefer to substitute the Ca^{2+} ions because the ionic radii of Ce^{3+} (1.14 Å) and Tb^{3+} (1.09 Å) are approximate to that of Ca^{2+} (1.12 Å).

$NaCaPO_4$ has an orthorhombic crystal structure with space group $Pn2_1a$, and the structure can be described as a superstructure of β-K_2SO_4.[23] As shown in Figure S1 in the Supporting Information, it is made up of two types of strings along the a axis, A and B. String A consists of alternating $[PO_4]$ tetrahedra and Na atoms. String B is made up of only Ca atoms, and Ca^{2+} has an eightfold coordination. The main difference between $NaCaPO_4$ and β-K_2SO_4 is the occurrence of three different orientations adopted here by the three independent $[PO_4]$ tetrahedra. The $[PO_4]$ tetrahedra have to change their orientations to accommodate the coordination requirements of the cations. In the crystal lattice, there are three types of eightfold-coordination Ca^{2+} sites. This means that Ce^{3+} ions could occupy three nonequivalent cation sites in $NaCaPO_4$. Although there are three Ca^{2+} sites, all Ca^{2+} ions are in an eightfold coordination with eight O^{2-} ions. In the emission spectra of $NaCaPO_4:Ce^{3+}$, the absence of distinct emission bands from different Ce^{3+} sites and both the peak position and the shape of the emission spectrum are independent of the excitation wavelength, thereby indicating a single type of luminescent center or strong spectral overlap between spectra that belong to different luminescent centers.[3]

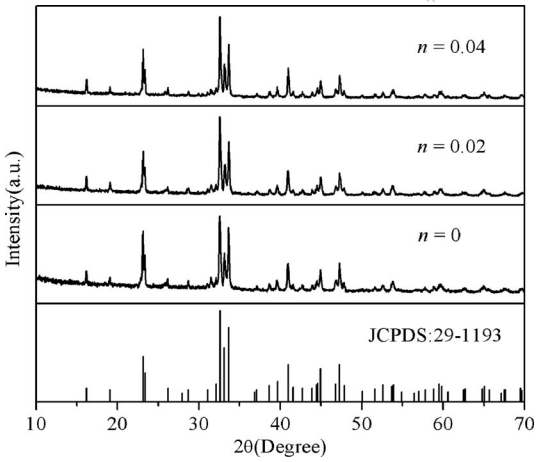

Figure 1. XRD profiles for $NaCaPO_4:0.02Ce^{3+},nTb^{3+}$ phosphors on Tb^{3+} doping content (n).

Optical Properties

The emission and excitation spectra of $NaCaPO_4:Ce^{3+}$ are presented in Figure 2. The Ce^{3+} singly doped sample exhibits an asymmetric band that extends from 340 to 450 nm with a maximum at about 370 nm when excited by 328 nm light and does not change with varying excitation

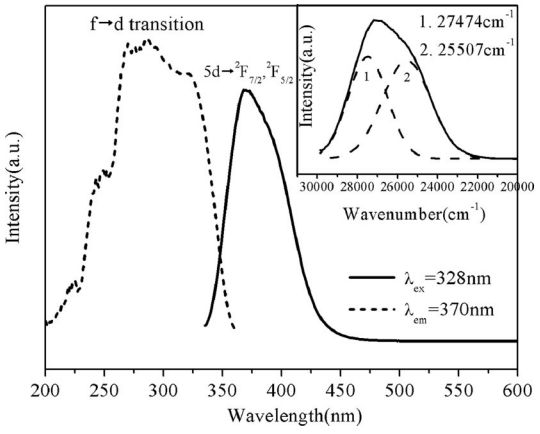

Figure 2. Excitation and emission spectra of the $NaCaPO_4:Ce^{3+}$ phosphor (λ_{ex} = 328 nm, λ_{em} = 370 nm). The inset shows the emission spectrum of $NaCaPO_4:0.02Ce^{3+}$ and the two Gaussian components on an energy scale.

wavelengths except for differences in intensity. The doublet bands due to the transition of the Ce^{3+} ions from the 5d excited state to the $^2F_{5/2}$ and $^2F_{7/2}$ ground states cannot be distinguished directly. However, the emission band can be decomposed into two well-separated Gaussian components with maxima at 27474 cm^{-1} (364 nm) and 25507 cm^{-1} (392 nm) on an energy scale with an energy difference of about 1967 cm^{-1} (inset in Figure 2), which is in agreement with the theoretical difference between the $^2F_{5/2}$ and $^2F_{7/2}$ levels (ca. 2000 cm^{-1}). The excitation spectrum of $NaCaPO_4:Ce^{3+}$ monitored at 370 nm shows several excitation bands in the region from 230 to 350 nm, which correspond to the transitions from the ground state to the $5d^1$ state of the field-splitting levels of the Ce^{3+} ions. The lowest excitation band is situated at 328 nm, so the Stokes shift of the Ce^{3+} emission is about 3461 cm^{-1}.

Figure 3 shows the excitation spectrum of the $NaCaPO_4:Tb^{3+}$ phosphor. The strong excitation bands are centered at 234 nm in the short-UV region within the range of 200–250 nm. It is well known that the ground state of the Tb^{3+} ion with a $4f^8$ electron configuration is on the $^7F_6$ level, and its $4f^75d^1$ excitation levels have high-spin (HS) ^9D_J and the low-spin (LS) ^7D_J states. As a result, a Tb^{3+} ion in a specific host exhibits two groups of f–d transitions; one group is spin-allowed with high energy, and another is spin-forbidden with low energy. Moreover, the energy difference [$\Delta E^{Tb,Ce} = E(Tb,A) - E(Ce,A)$] between this first f–d transition of the Tb^{3+} ion (234 nm, 42735 cm^{-1}) and that of the Ce^{3+} ion (328 nm, 30488 cm^{-1}) is 12247 cm^{-1}; it is near the average value of 13200 cm^{-1} for the spin-allowed f–d transition of the Tb^{3+} ions. The energy difference between the bands at 234 and 273 nm is 6105 cm^{-1}, which is near the average energy difference between the spin-allowed f–d transition with that of the spin-forbidden transition for the Tb^{3+} ion (6300 cm^{-1}).[24] Therefore, the band at 234 nm is assigned to the first spin-allowed (low-spin) f–d transition of the Tb^{3+} ions, and the relatively weak band at 273 nm is due to the spin-forbidden (high-spin) transitions of the Tb^{3+} ions that involve the $4f^8$ and $4f^75d$ electronic configurations in the ground and excited states. Besides this, there are several excitation bands between 280 and 400 nm due to the intra-$4f^8$ transitions from the $^7F_6$ to the $^5F_{5,4}$, $^5H_{7-4}$, $^5D_{1,0}$, $^5L_{10-7}$, $^5G_{6-2}$, and $^5D_{2-3}$ levels. As shown in Figure 4, the Tb^{3+} emission peaks at 489, 544, 583, and 620 nm are assigned to the $^5D_4$ to ^7F_J (J = 6, 5, 4, 3) transitions, respectively. Among them, the green emission of the $^5D_4 \rightarrow {}^7F_5$ transition at 544 nm is clearly predominant at higher Tb^{3+} concentrations, which can be elucidated by the large values of the reduced matrix elements at J = 5 and the Judd–Ofelt theory.[25,26] It is clear that the $NaCaPO_4:Tb^{3+}$ phosphor is optimally excited at 234 nm. One can note from Figure 4 that the spectral-energy distribution of the Tb^{3+} emission depends strongly on the Tb^{3+} concentration. It is clear that the emission spectra show different ratios between the $^5D_3$ and the $^5D_4$ emissions at lower and higher Tb^{3+} concentrations. The emission spectrum for low Tb^{3+} concentrations consists of the transitions from both the $^5D_3$ and $^5D_4$ levels. With an increase in the Tb^{3+} concentration, the emissions from the $^5D_3$ to the ^7F_J levels are quenched gradually by the cross-relaxation process between neighboring Tb^{3+} ions. This is the process whereby excitation energy from an ion that is decaying from a highly excited state promotes a nearby ion from the ground state to the metastable level. For the Tb^{3+} ion, the energy gap between the $^5D_3$ and $^5D_4$ levels is close to that between the $^7F_6$ and $^7F_0$ levels. As a result, if the Tb^{3+} concentration is high enough, the higher-energy-level emission can be easily quenched in favor of the lower-energy-level emission. This cross-relaxation process produces the rapid population of the $^5D_4$ level at the expense of the $^5D_3$ level, thereby resulting in a strong emission from the $^5D_4$ to the ^7F_J levels.

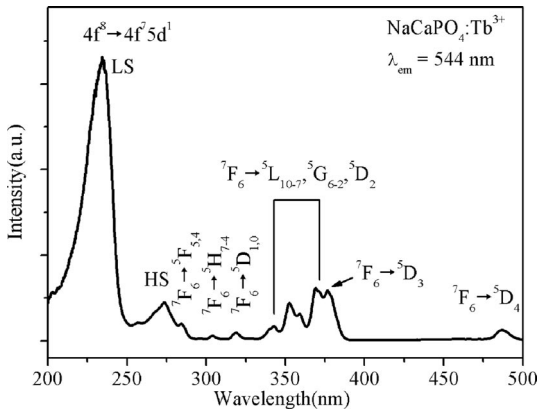

Figure 3. Excitation spectrum of the $NaCaPO_4:Tb^{3+}$ phosphor (λ_{em} = 544 nm).

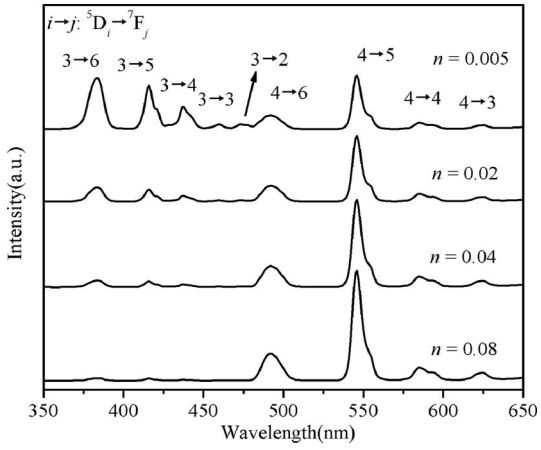

Figure 4. Emission spectra of the $NaCaPO_4:nTb^{3+}$ phosphor (λ_{ex} = 234 nm).

In this work, our aim is to verify whether the Ce^{3+} ions can further enhance the luminescence intensity of the Tb^{3+} ions. The corresponding energy-transfer mechanism has also been investigated in this work. As shown in Figures 2 and 3, the comparison of the emission and excitation spectra for the $NaCaPO_4:Ce^{3+}$ and $NaCaPO_4:Tb^{3+}$ phosphors reveals a significant spectral overlap between the emission band of the Ce^{3+} ions and the excitation band of the Tb^{3+} ions. Therefore, it is expected that an efficient resonance-

type energy transfer can occur from the Ce^{3+} to the Tb^{3+} ions. This type of energy transfer is quite common and has been observed in several Ce^{3+}- and Tb^{3+}-coactivated phosphors such as Al_2O_3-B_2O_3:Ce^{3+},Tb^{3+},[15] YPO_4:Ce^{3+},Tb^{3+},[17] $Ca_2Al_2SiO_7$:Ce^{3+},Tb^{3+},[18] and $LaPO_4$:Ce^{3+},Tb^{3+},[19] respectively.

Figure 5 shows the excitation and emission spectra of $NaCaPO_4$:0.02Ce^{3+},nTb^{3+} phosphors. The excitation spectrum monitored at 370 nm (Ce^{3+} emission) shows several excitation bands, which are attributed to the $4f^1 \rightarrow 5d^1$ transition of the Ce^{3+} ions. Under excitation at 328 nm, the emission spectra of $NaCaPO_4$:0.02Ce^{3+},nTb^{3+} appear not only as a band of Ce^{3+} ions but also as an intense green band of Tb^{3+} ions. With an increase in Tb^{3+} content (n), the emission intensity of the Tb^{3+} ions increases systematically, whereas the emission intensity of the Ce^{3+} ions simultaneously decreases monotonically from n = 0.02 to 0.08. The excitation spectrum monitored at 544 nm consists of the excitation bands of the Ce^{3+} and Tb^{3+} ions, which means that the Tb^{3+} ions are essentially excited through the Ce^{3+} ions, thereby indicating efficient energy transfer from the Ce^{3+} to Tb^{3+} ions (Figure 5a). The 5d–4f transition of Ce^{3+} is electric-dipole-allowed and is several orders of magnitude stronger than the f–f transitions of Tb^{3+}. Therefore, the Ce^{3+} ions can strongly absorb UV light from the ground states to the excited states, and then efficiently transfer the energy to the Tb^{3+} ions. As a result, the excitation into the Ce^{3+} band at 328 nm yields both the emissions of the Ce^{3+} and Tb^{3+} ions. Since the electronic transitions within $4f^n$ configurations of Tb^{3+} ions are strongly forbidden, they appear in the absorption spectrum with very weak intensity. However, the excitation that results in high light output can be achieved by exciting a sensitizer with an allowed electronic transition that transfers the excitation energy to the activator. In this case, it is the energy transfer from the Ce^{3+} to Tb^{3+} ions that leads to highly efficient green emission of the Tb^{3+} ions.

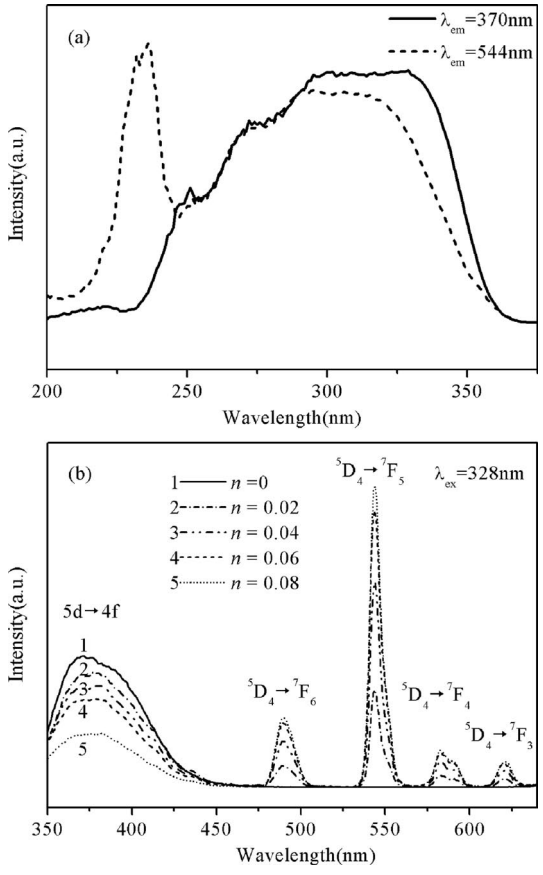

Figure 5. Excitation spectra of $NaCaPO_4$:0.02Ce^{3+},0.02Tb^{3+} monitored at (a) 370 and 544 nm; (b) emission spectra of $NaCaPO_4$:0.02Ce^{3+},nTb^{3+} phosphors.

We were also interested in investigating the energy-transfer efficiency (η_T) from the Ce^{3+} to the Tb^{3+} ions. The energy-transfer efficiency from a sensitizer to an activator can be calculated by Equation (1):[27]

$$\eta_T = 1 - \frac{I_S}{I_{S0}} \quad (1)$$

in which I_S and I_{S0} are the luminescence intensities of the sensitizer (Ce^{3+}) with and without the activator (Tb^{3+}) present, respectively. The η_T value of $NaCaPO_4$:0.02Ce^{3+},nTb^{3+} could be obtained as a function of n and is presented in Figure 6, in which η_T was found to increase gradually with an increase in Tb^{3+} dopant content.

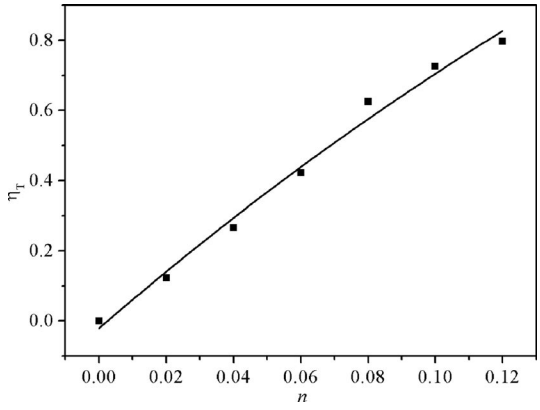

Figure 6. Dependence of the energy-transfer efficiency η_T in $NaCaPO_4$:Ce^{3+},Tb^{3+}on the Tb^{3+} content (n).

In many cases, concentration quenching is due to the energy transfer from one activator to another until the energy sink in the lattice is reached.[28] Blasse suggested that the average separation R_{Ce-Tb} of energy transfer can be estimated from Equation (2):[21]

$$R_{Ce-Tb} \approx 2\left[\frac{3V}{4\pi x N}\right]^{1/3} \quad (2)$$

in which V is the volume of the unit cell, N is the number of the host cations in the unit cell, and x is the total concentration of Ce^{3+} and Tb^{3+} ions. The critical concentration (x_c) is that at which the luminescence intensity of sensitizer (Ce^{3+}) is half that in the sample in the absence of activator (Tb^{3+}), that is to say, x_c occurs when η_T = 0.5. For the

$NaCaPO_4$ host, N is 4 and V is estimated to be 336.76 Å^3 with the assumption that the lattice parameters are almost constant with Ce^{3+} and Tb^{3+} doping levels. The critical distance of energy transfer R_c is estimated to be about 12.1 Å from the total concentration of Ce^{3+} (= 0.02) and Tb^{3+} (= 0.07) at which the energy-transfer efficiency is 0.5 (Figure 6).

Figure 7 shows the decay curves of the $^5D_4 \rightarrow {}^7F_5$ transition of the Tb^{3+} ions in $NaCaPO_4$:$m$$Ce^{3+}$,0.02$Tb^{3+}$ with different Ce^{3+} concentrations. For the decay curves of the Tb^{3+} ions, the decays show nonexponential curves, which can be calculated by the effective lifetime as Equation (3):[29]

$$\tau_{average} = \frac{\int_0^\infty I(t)tdt}{\int_0^\infty I(t)dt} \quad (3)$$

in which $I(t)$ represents the luminescence intensity at a time t. The decay times of the Tb^{3+} ions are prolonged when Ce^{3+} ions are doped. The result further testifies that there exists energy transfer from the Ce^{3+} to the Tb^{3+} ions.

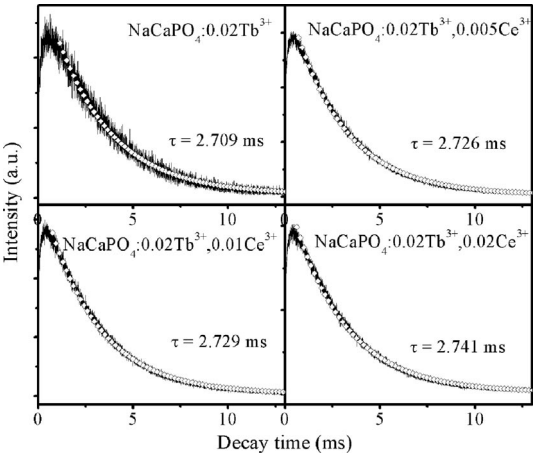

Figure 7. Fluorescence-decay curves for the $^5D_4 \rightarrow {}^7F_5$ transition of Tb^{3+} in the phosphors with 0, 0.5, 1, and 2% Ce^{3+} (the Tb^{3+} content is fixed at 2%). The solid lines are the experimental data, and scattered points are the fitted curves (λ_{ex} = 328 nm).

The energy transfer from a sensitizer to an activator may take place through radiative transfer, exchange interaction, and electric multipolar interaction. The absence of the dips in the emission peak of the Ce^{3+} ions that correspond to the f–f absorption lines of the Tb^{3+} ions shows that radiative energy transfer between the donor and the acceptor can be neglected. Exchange interaction needs a large direct or indirect overlap between donor and acceptor orbitals to lead to easy electronic exchange. Although both Ce^{3+} and Tb^{3+} ions are reducing ions, such an exchange would require energies that were too high.[20] Therefore energy transfer through exchange interaction is impossible. Thus, the energy transfer in $NaCaPO_4$ takes place by means of an electric multipolar interaction. The transition of the Ce^{3+} ions from the 5d excited state to the $^2F_{5/2}$ and $^2F_{7/2}$ ground states are pure electric dipolar transitions, but the $4f^8$–$4f^8$ Tb^{3+} transitions have simultaneously dipolar and quadrupolar character. Therefore, both dipole–dipole and dipole–quadrupole mechanisms may be involved in the energy transfer from the Ce^{3+} to Tb^{3+} ions. According to Dexter's energy-transfer formula of multipolar interaction and Reisfeld's approximation, Equation (4) can be given:[12,21]

$$\frac{\eta_{S0}}{\eta_S} \propto C_{Ce+Tb}^{n/3} \quad (4)$$

in which η_{S0} is the intrinsic luminescence quantum efficiency of the Ce^{3+} ions and η_S is the luminescence quantum efficiency of the Ce^{3+} ions with the activator (Tb^{3+}) present; the values of η_{S0}/η_S can be approximately calculated by the ratio of related luminescence intensities (I_{S0}/I_S); C_{Ce+Tb} is the total dopant concentration of Ce^{3+} and Tb^{3+}; and the n = 6, 8, and 10, are dipole–dipole, dipole–quadrupole, and quadrupole–quadrupole interactions, respectively.

The I_{S0}/I_S–$C^{n/3}$ plots are further illustrated in Figure 8a–c, and the relationships are observed when n = 6, 8, and 10. Only when n = 8 does it show a linear relation. This clearly indicates that the energy transfer from the Ce^{3+} to the Tb^{3+} ions is the dipole–quadrupole mechanism. Therefore, the electric dipole–quadrupole interaction predominates in the energy-transfer mechanism from the Ce^{3+} to the Tb^{3+} ions in $NaCaPO_4$:Ce^{3+},Tb^{3+}, which is similar to the results in the literature.[20,30]

To further investigate the characteristics of multipolar interactions such as dipole–dipole, dipole–quadrupole, and higher-order interactions, the energy-transfer probability P_{SA} [s^{-1}] for each multipolar interaction was considered.[21] The dipole–dipole energy-transfer probability (P_{SA}) from a sensitizer to an acceptor is given by Equation (5):[12,21]

$$P_{Ce-Tb}^{dd} = 3.024 \times 10^{12} \frac{f_d}{R^6 \tau_S} \int \frac{F_S(E)F_A(E)dE}{E^4} \quad (5)$$

in which f_d is the oscillator strength of the involved absorption transition of the acceptor, τ_S is the radiative decay time of the sensitizer [s], R is the sensitizer–acceptor average distance [Å], E is the energy involved in the transfer [eV], and $\int F_S(E)F_A(E)/E^4dE$ represents the spectral overlap between the normalized shapes of the Ce^{3+} emission $F_S(E)$ and the Tb^{3+} excitation $F_A(E)$, and in our case it is calculated to be about 0.01186 eV^{-5}. The critical distance (R_c) of the energy transfer from the sensitizer to the acceptor is defined as the distance for which the probability of transfer equals the probability of radiative emission of donor, the distance for which $P_{Ce-Tb}\tau_{S0}$ = 1. Hence, R_c can be obtained from Equation (6):

$$R_C^6 = 3.024 \times 10^{12} f_d \int \frac{F_S(E)F_A(E)dE}{E^4} \quad (6)$$

The oscillator strength of the Tb^{3+} electric dipole transition (f_d) is in the order of 10^{-6}.[20] From the above equation, by using this value and the calculated spectral overlap, the

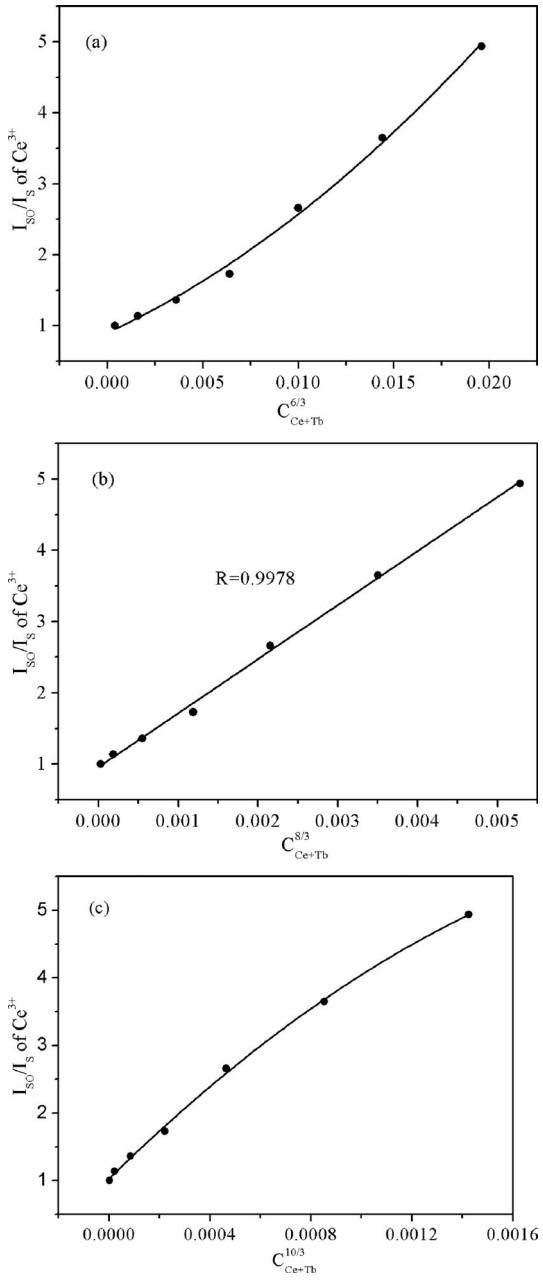

Figure 8. Dependence of I_{S0}/I_S of Ce^{3+} on (a) $C^{6/3}$, (b) $C^{8/3}$, and (c) $C^{10/3}$.

critical distance R_c^{dd} for a dipole–dipole interaction mechanism is calculated as 5.7 Å. This value largely deviates from that estimated from the quench concentration data (12.1 Å), thus further indicating that the electric dipole–dipole interaction is not primarily responsible for the energy transfer from the Ce^{3+} to the Tb^{3+} ions. Therefore, we should consider an electric dipole–quadrupole interaction as a possible mechanism for an energy transfer.

The relationship of the transfer probability between P^{dq} of the dipole–quadrupole interaction and P^{dd} of the dipole–dipole interaction is given by Equation (7):

$$\frac{P^{dq}}{P^{dd}} \approx \left(\frac{\lambda_S}{R}\right)^2 \frac{f_q}{f_d} \quad (7)$$

in which λ_S [Å] is the wavelength position of the sensitizer's emission, and f_d and f_q are the oscillator strengths of the electric dipole and quadrupole transitions, respectively. Using Equations (5) and (7), we obtain Equation (8):

$$R_C^8 = 3.024\times10^{12}\,\lambda_S^2 f_q \int \frac{F_S(E)F_A(E)dE}{E^4} \quad (8)$$

It is a pity that the oscillator strength of the Tb^{3+} quadrupole transition (f_q) has not been obtained up to now. However, it was suggested by Verstegen et al. that the ratio f_q/f_d is about 10^{-3}–10^{-2}.[20] From Equation (8), by using these values and the calculated spectral overlap, the critical distance R_c^{dd} for a dipole–quadrupole interaction mechanism is 12.2–16.3 Å. The critical distance R_c^{dd} was estimated to be 12.2 Å, which agrees approximately with that obtained by using the concentration-quenching method (12.1 Å). This result allows us to conclude for the first time that the more reasonable ratio f_q/f_d for the Tb^{3+} ion is about 10^{-3}.

For modern white-light LED applications, the quantum efficiency (*QE*) is an important parameter for LED phosphors. So the efficiency of the phosphors is important and necessary. The obtained external *QE* of NaCaPO$_4$:0.02Ce^{3+},0.02Tb^{3+}; NaCaPO$_4$:0.02Ce^{3+},0.04Tb^{3+}; and NaCaPO$_4$:0.02Ce^{3+},0.06Tb^{3+} are 49.1, 76.2, and 74.7%, respectively. The value of *QE* is somewhat lower than that of LaPO4:Ce^{3+},Tb^{3+} (86%).[31] However, it should be noted that its excitation-wavelength range fits with the characteristic emission of UV-LED chips based on AlGaN, whereas LaPO$_4$:Ce^{3+},Tb^{3+} is not suitable for the excitation of UV-LEDs due to the limitation of the excitation-wavelength range. The developed phosphors have the advantages of appropriate emission efficiency and relatively low price.

The Commission Internationale de L'Eclairage (CIE) chromaticity coordinates for NaCaPO$_4$:0.02Ce^{3+},*n*Tb^{3+} excited under 328 nm are presented in Figure S2 in the Supporting Information. With an increase in Tb^{3+} content, the chromaticity coordinates (*x*, *y*) vary systematically from (0.17, 0.03) to (0.27, 0.38) and ultimately to (0.32, 0.56), thus the corresponding color tone of the samples changes gradually from blue to green and eventually to yellow-greenish. We have obtained a green color for NaCaPO$_4$:0.02Ce^{3+},0.02Tb^{3+}; its chromaticity coordinates were calculated as (0.27, 0.38). The phosphor emits green light during excitation with a UV wavelength of 328 nm, which is accessible by UV LEDs based on AlGaN.[32] This result indicates that this phosphor might serve as a potential green-emitting UV-convertible phosphor under UV excitation.

Conclusion

We have synthesized $NaCaPO_4:Ce^{3+},Tb^{3+}$ phosphors and investigated their luminescence. The spectroscopic data indicate that the energy transfer from the Ce^{3+} to the Tb^{3+} ions takes place in the host matrix of $NaCaPO_4$. The mechanism of the energy transfer is a resonant type that takes place through a dipole–quadrupole reaction. The green emission of the Tb^{3+} ions is observed in $NaCaPO_4:Ce^{3+},Tb^{3+}$ upon UV excitation due to the energy transfer from the Ce^{3+} to the Tb^{3+} ions. The efficiencies from the Ce^{3+} to Tb^{3+} ions were calculated by the changes of their relative emission intensity. The critical distance of the energy transfer is about 12.1 Å. Furthermore, we have demonstrated that the $NaCaPO_4:Ce^{3+},Tb^{3+}$ phosphors can be tuned to generate green light under UV radiation. Preliminary studies have shown that the $NaCaPO_4:Ce^{3+},Tb^{3+}$ phosphor may serve as a potential green-emitting UV-convertible phosphor under UV excitation. More importantly, the obtained accurate ratio f_q/f_d for the Tb^{3+} ion may open a way to calculate the critical distance of the dipole–quadrupole interaction between the Ce^{3+} and the Tb^{3+} ions in other luminescent materials.

Experimental Section

Materials and Synthesis: Na_2CO_3 (A.R.), $CaCO_3$ (A.R.), $NH_4H_2PO_4$ (A.R.), CeO_2 (99.99%), and Tb_4O_7 (99.99%) were used as the starting materials. The phosphors with nominal composition of $NaCa_{1-m-n}PO_4:mCe^{3+},nTb^{3+}$ were synthesized through a solid-state reaction technique. The stoichiometric amounts of the raw materials were first thoroughly mixed by grinding them in an agate mortar. The resulting mixture was placed in a small covered crucible, which was then transferred to a large crucible. The space between the two crucibles was filled with powdered graphite. Then, the large crucible was placed in a muff furnace under ambient atmosphere and fired at 900 °C for 3 h. Finally, the large crucible was cooled to room temperature and a fine powder was obtained.

Characterization: Powder X-ray diffraction (XRD) measurements were performed with a D8 Focus diffractometer (Bruker) at a scanning rate of 15 ° min^{-1} in the 2θ range from 10 to 80°, with graphite-monochromatized Cu-K_α radiation (λ = 0.15405 nm) operating at 40 kV and 40 mA. The photoluminescence excitation and emission spectra of the obtained powders were recorded with a Hitachi F-4500 spectrophotometer equipped with a 150 W xenon lamp as the excitation source. The external quantum efficiency (*QE*) was analyzed with a PL quantum-efficiency measurement system (C9920-02, Hamamatsu Photonics, Shizuoka) under excitation at 325 nm by a 150 W xenon lamp. The luminescence decay curve was obtained from a Lecroy Wave Runner 6100 digital oscilloscope (1GHz) by using a tunable laser (pulse width = 4 ns, gate = 50 ns) as the excitation source (Continuum Sunlite OPO). All the measurements were carried out at room temperature.

Supporting Information (see footnote on the first page of this article): Projection of the crystal structure of $NaCaPO_4$ and the local coordination tetrahedron of $[PO_4]$, viewed along [010] and [100]; CIE chromaticity diagram for $NaCaPO_4:0.02Ce^{3+},nTb^{3+}$ excited at 328 nm. (1) n = 0; (2) n = 0.02; (3) n = 0.04; (4) n = 0.06; (5) n = 0.08.

Acknowledgments

This work was financially supported by the National Natural Science Foundation of China (grant no. 20771098), the Fund for Creative Research Groups (grant no. 20921002), and the National Basic Research Program of China (973 Program, grant nos. 2007CB935502 and 2006CB601103).

[1] R. J. Xie, N. Hirosaki, M. Mitomo, K. Sakuma, N. Kimura, *Appl. Phys. Lett.* **2006**, *89*, 241103.
[2] J. S. Kim, P. E. Jeon, J. C. Choi, H. L. Park, S. I. Mho, G. C. Kim, *Appl. Phys. Lett.* **2004**, *84*, 2931.
[3] Y. H. Song, G. Jia, M. Yang, Y. J. Huang, H. P. You, H. J. Zhang, *Appl. Phys. Lett.* **2009**, *94*, 091902.
[4] K. Inoue, N. Hirosaki, R. J. Xie, T. Takeda, *J. Phys. Chem. C* **2009**, *113*, 9392–9397.
[5] Y. Q. Li, A. C. A. Delsing, G. D. With, H. T. Hintzen, *Chem. Mater.* **2005**, *17*, 3242–3248.
[6] C. X. Qin, Y. L. Huang, L. Shi, G. Q. Chen, X. B. Qiao, H. J. Seo, *J. Phys. D: Appl. Phys.* **2009**, *42*, 185105.
[7] Z. C. Wu, J. Liu, M. L. Gong, Q. Su, *J. Electrochem. Soc.* **2009**, *156*, H153.
[8] Z. P. Yang, G. W. Yang, S. L. Wang, J. Tian, X. N. Li, Q. L. Guo, G. S. Fu, *Mater. Lett.* **2008**, *62*, 1884–1886.
[9] Z. C. Wu, J. X. Shi, J. Wang, M. L. Gong, Q. Su, *J. Solid State Chem.* **2006**, *179*, 2356–2360.
[10] Y. S. Tang, S. F. Hu, C. C. Lin, N. C. Bagkar, R. S. Liu, *Appl. Phys. Lett.* **2007**, *90*, 151108.
[11] T. S. Chan, R. S. Liu, I. Baginskiy, *Chem. Mater.* **2008**, *20*, 1215–1217.
[12] D. L. Dexter, *J. Chem. Phys.* **1953**, *21*, 836–850.
[13] G. Blasse, *Chem. Mater.* **1989**, *1*, 294–301.
[14] B. M. Smets, *Mater. Chem. Phys.* **1987**, *16*, 283–299.
[15] H. P. You, G. Y. Hong, X. Y. Wu, *Chem. Mater.* **2003**, *15*, 2000–2004.
[16] S. Nigam, V. Sudarsan, R. K. Vatsa, *J. Phys. Chem. C* **2009**, *113*, 8750–8755.
[17] H. Lai, A. Bao, Y. M. Yang, Y. C. Tao, H. Yang, Y. Zhang, L. L. Han, *J. Phys. Chem. C* **2008**, *112*, 282–286.
[18] H. Y. Jiao, Y. H. Wang, *J. Electrochem. Soc.* **2009**, *156*, J117.
[19] I. W. Lenggoro, B. Xia, H. Mizushima, K. Okuyama, N. Kijima, *Mater. Lett.* **2001**, *50*, 92.
[20] J. M. P. J. Verstegen, J. L. Sommerdijk, J. G. Verriet, *J. Lumin.* **1973**, *6*, 425–431.
[21] G. Blasse, *Philips Res. Rep.* **1969**, *24*, 131.
[22] R. D. Shannon, *Acta Crystallogr., Sect. A* **1976**, *32*, 751.
[23] M. B. Amara, M. Vlasse, G. L. Flem, P. Hagenmuller, *Acta Crystallogr., Sect. C* **1983**, *39*, 1483–1485.
[24] P. Dorenbos, *J. Lumin.* **2000**, *91*, 155.
[25] B. R. Judd, *Phys. Rev.* **1962**, *127*, 750.
[26] G. S. Ofelt, *J. Chem. Phys.* **1962**, *37*, 511.
[27] P. I. Paulose, G. Jose, V. Thomas, N. V. Unnikrishnan, M. K. R. Warrier, *J. Phys. Chem. Solids* **2003**, *64*, 841.
[28] D. L. Dexter, J. A. Schulman, *J. Chem. Phys.* **1954**, *22*, 1063.
[29] F. Lahoz, I. R. Martin, J. Mendz-Ramos, P. Nunez, *J. Chem. Phys.* **2004**, *120*, 6180.
[30] W. J. Yang, L. Luo, T. M. Chen, N. S. Wang, *Chem. Mater.* **2005**, *17*, 3883.
[31] Z. X. Fu, W. B. Bu, *Solid State Sci.* **2008**, *10*, 1062.
[32] A. Höppe, M. Daub, M. C. Bröhmer, *Chem. Mater.* **2007**, *19*, 6358.

Received: April 9, 2010
Published Online: August 17, 2010

